学 位 論 文（要約）

Studies on morphogenesis of floral organ of the dioecious *Silene latifolia* and the smut fungus *Microbotryum lychnidis-dioicae* disturbing it

(雌雄異株植物ヒロハノマンテマの花器官の形態形成とそれを撹乱する黒穂菌に関する研究**)**

平成 **28** 年 **12** 月　博士（生命科学）申請

東京大学大学院新領域創成科学研究科

先端生命科学専攻

川元　寛章

Studies on morphogenesis of floral organ of the dioecious *Silene latifolia* and the smut fungus *Microbotryum lychnidis-dioicae* disturbing it

Hiroki Kawamoto

2016

Department of Integrated Biosciences

Graduate School of Frontier Sciences

The University of Tokyo

ACNOWLEDGMENTS

I would like to first express my gratitude to Professor Shigeyuki Kawano of the University of Tokyo for kind instruction and continuous encouragement throughout in this study. I further wish to express thanks to Dr. Aiko Hirata of The University of Tokyo and Ms. Kyoko Kudo for teaching me serial sectioning methods of transmission electron microscopy. I express my gratitude to Dr. Wakana Tanaka of The University of Tokyo for teaching me *in situ* hybridization. I am also grateful to Dr. Yusuke kazama and Dr. Kotarou Ishii Dr. Tomoko Abe of RIKEN, Dr. Ayako koizumi and Ms. Kaori yamanaka for helpful discussions and supports. I thank Dr. Michael E. Hood for kind instruction on the preparation of *Microbotryum lychnidis-dioicae.*

I express my gratitude to Professor Seiichiro Hasezawa, Professor Masashi Ugaki, Associate Professor Kuninori Suzuki of the Department of Frontier Sciences, University of Tokyo, and Professor Hiro-Yuki Hirano, Department of Biological science, University of Tokyo, for useful suggestions and discussions in this study. I am also grateful to Dr. Shuhei Ota, Dr. Tomokazu Yamazaki, Dr. Kensuke Ichihara, Dr. Tsuyoshi Takeshita, Ms. Madoka Asano, and Ms. Aya Morita for support, kindness, and encouragement throughout this study. Finally, I wish to thank all of my family for their mental and physical support and constant encouragement.

CONTENTS

CONTENTS

ABBREVIATION

DAPI	4',6-diamidino-2-phenylindole
DNA	deoxyribonucleic acid
FITC	fluorescein isothiocyanate
GSF	gynoecium-suppressing function
ISH	in situ hybridization
MFF	male-fertility function
PCR	polymerase chain reaction
RAPD	random amplified polymorphic DNA
RFLP	restriction fragment length polymorphism
RNA	ribonucleic acid
SEM	scanning electron microscopy
SPF	stamen-promoting function
TEM	transmission electron microscopy
TUNEL	terminal deoxynucleotidyl transferase dUTP nick end labeling

PREFACE

Organisms developed sexuality to maintain species diversity during evolution over the long term. Sexuality is acquired independently during speciation because, although sexuality is common among animal species, the sex-determining mechanisms are not common among animal species (Charlesworth 2016).

Unlike most animal species, flowering plants can be hermaphroditic and develop bisexual flowers. Hermaphroditic flowers, which have both gynoecium and stamens, bloom in most flowering plants. However, unisexual flowers bloom in approximately 10% of flowering plants (Ainsworth 2000). Half these species are diclinous plants, which have male and female flowers in the same plant. The other half are dioecious plants, which have male and female flowers in different plants (Charlesworth and Guttman 1999). These strategies did not evolve from a single hermaphroditic ancestor, although dioecious and monoecious plants broadly exist in orders or families (Renner 2014; Fig. P-1). Many plant species have stamens and gynoecium during early floral organ developmental stages. Therefore, hermaphrodites are the ancestral type, and dioeciousism and monoeciousism were created through developmental suppression, which occurs at the stamen or gynoecium in a hermaphroditic flower (Diggle et al., 2011). Molecular and genetic studies have been

carried out to determine the mechanism of sex determination in several dioecious plants.

The genus *Silene* includes hermaphroditic, gynodioecious, and dioecious plants with stamens and gynoecium in flowers of the same plant (Desfeux et al., 1996). A gynodioecious plant has female flowers and bisexual flowers in the same individual. A dioecious plant has female and male flowers in the same individual. However, only dioecious plants have sex chromosomes in these phenotypes. Therefore, it is thought that sexuality and sex chromosomes evolved independently in family Caryophyllaceae. *Silene latifolia* evolved from a hermaphroditic ancestor 800 to 24 million years ago, and the XY type sex chromosome was acquired at that time (Desfeux et al., 1996; Charlesworth 2002). As mammalian sex chromosomes were acquired about 300 million years ago, the *S. latifolia* sex chromosome is extremely new. Dr. Charlesworth has suggested that the establishment of the Y chromosome from a hermaphrodite is necessary for a deficiency in the stamen developmental function and for the dominant mutation of the developmental suppression of the gynoecium function (Charlesworth et al., 1978). The male-determining factor that promotes development of the stamen exists on the *S. latifolia* Y chromosome (Kazama et al., 2016). As the male-determining factor is present only on the Y chromosome, females with only an X chromosome have no ability to develop stamens. However, when *Microbotryum lychnidis-dioicae* is infected

with female flowers, stamens in the female flower develop like male flowers (Uchida et al., 2013). It is thought that *M. lychnidis-dioicae* replaces the Y chromosome, as stamens develop in the female flower after infection with *M. lychnidis-dioicae*. The genetic program that determines sex-specific development of stamens and gynoecium, as seen in *S. latifolia*, is thought to involve regulation of factors that pattern tissue formation (Matsunaga et al., 2004).

The plant sex-determining gene was first identified in *Diospyros lotus* in 2014 (Akagi et al., 2014). The sex-determining mechanism of persimmon involves a dominant Y chromosome, which is thought to be the case for *S. latifolia*. A combination of transcriptomic and evolutionary approaches detected OGI as a Y-specific sex-determinant candidate, as it displays male-specific conservation in the genus *Diospyros*. OGI encodes a small RNA targeting the autosomal MeGI gene, which is a homeodomain transcription factor regulating anther fertility in a dose-dependent fashion.

As the sex-determining system in animals varies among species, various sex-determining systems exist in plants as well. It is necessary to identify and compare the sex-determining genes and sex-determining systems in various plant species to investigate the origin of plant sex-determining systems. In this study, the mechanism for

S. latifolia sexuality is investigated using *M. lychnidis-dioica*e, which morphologically disturbs the sex-determining system of *S. latifolia*.

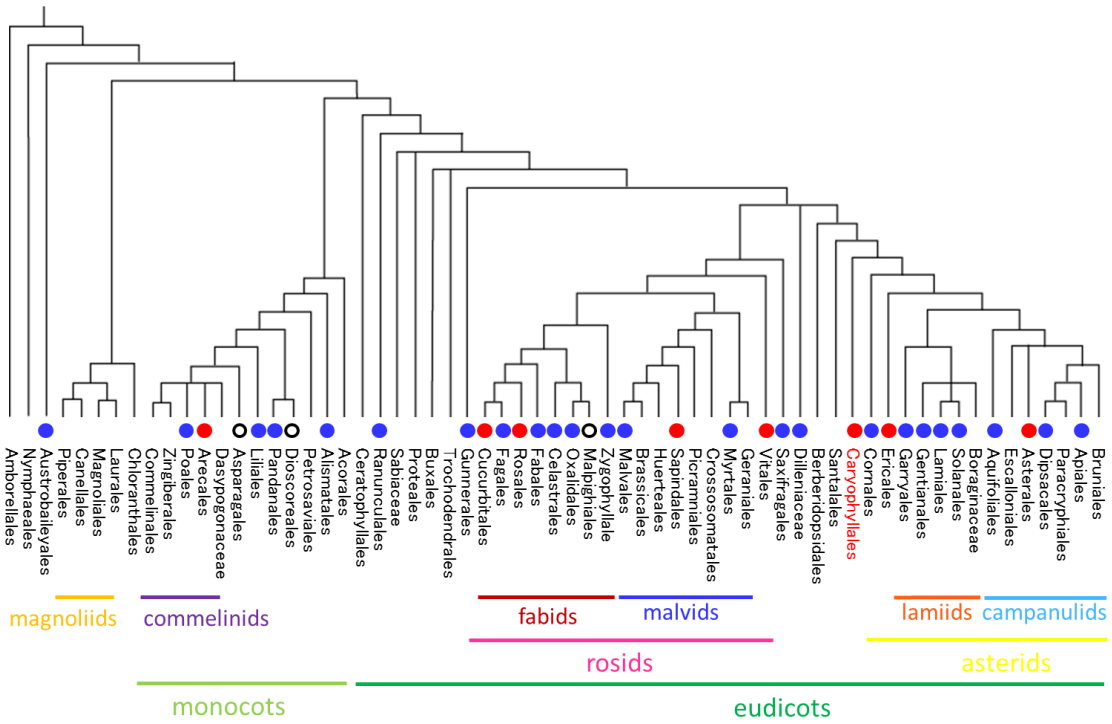

Fig. P-1 Interrelationships of the Angiosperm Phylogeny Group III orders and sex chromosomes in angiosperms. This figure combine the analysis of Charlesworth et al., (2002) and the phylogenetic analysis of Bremer, et al. (2009). Red circle indicates the presence of species, which have heteromorphic sex chromosomes. Blue circle indicates the presence of dioecy. White circle indicates that sex chromosomes are believed to be absent in spite of the presence of dioecy. Highlighted red indicates Caryophyllales, which including *S. latifolia*.

CHAPTER I

Cell death and cell cycle arrest of *Silene latifolia* stamens and pistils after *Microbotryum lychnidis-dioicae* infection

SUMARRY

Mechanisms of pistil primordia suppression in male flowers and stamen primordia suppression in female flowers differ in diclinous plants. In this study, I investigated how cell death and cell cycle arrest are related to flower organ formation in *S. latifolia*. Using *in situ* hybridization and a TUNEL assay, I detected both cell cycle arrest and cell death in suppressed stamens of female flowers and suppressed pistils of male flowers in *S. latifolia*. In female flowers infected with *M. lychnidis-dioicae*, developmental suppression of stamens is released, and cell cycle arrest and cell death do not occur. Smut spores are formed in *S. latifolia* anthers infected with *M. lychnidis-dioicae*, followed by cell death in the endothelium, middle layer, tapetal cells and pollen mother cells. Cell death is difficult to detect using an FITC-labeled TUNEL assay due to strong auto-fluorescence in the anther. I therefore combined a TUNEL assay in an infrared region with transmission electron microscopy to detect cell death in anthers. I show that following infection by *M. lychnidis-dioicae*, a TUNEL signal was not detected in the endothelium, middle layer, or pollen

mother cells, and cell death with outflow of cell contents, including the nucleoplast, was observed in tapetal cells.

INTRODUCTION

Hermaphroditic flowers, which have both pistils and stamens, blossom in most flowering plants. However, unisexual flowers blossom only in approximately 10% of flowering plants（Ainsworth 2000). Half of these are diclinous plants, as they have male and female flowers in the same plant. The other half are dioecious plants, as they have male and female flowers in individual plants (Charlesworth and Guttman 1999). Most of the diclinous and dioecious plants have stamen and pistil primordia during their early developmental stages.

In later stages, the anther is suppressed until maturity in the female flower, whereas the pistil is suppressed until maturity in the male flower (Ainsworth 2000; Mitchell and Diggle 2005). The timing of stamen and pistil suppression differs among species. When stamen and pistil primordia are formed in the *Zea mays* and *Cucumis sativus* of the diclinous plants, developmental suppression occurs in the pistils of male flowers and in the stamens of female flowers (Calderson-Urrea and Dellaporta 1999; Bai et al., 2004). On the other hand, when stamens form pollen in the female flowers

and pistils form an embryo sac in the male flowers in *Opuntia stenopetala* diclinous plants, developmental suppression occurs in the pistils of the male flowers and in the stamens of the female flowers (Strittmatter et al., 2006; Flores-Rentería et al., 2011).

It is thought that suppression related to male and female flower formation involves two mechanisms. One mechanism is cell cycle arrest in specific organs, and the other is cell death, also in specific organs (Diggle et al., 2011). *In situ* hybridization using histone and cyclin probes is effective for detecting the activity of cell division in suppression organs (Matsunaga et al., 2004; Kim et al., 2007; Daher et al., 2010). Cells that express the cyclin and histone genes undergo cell division. Histone genes are expressed in the DNA synthetic period and endoreduplication, and cyclin genes are expressed in the DNA synthetic and Gap 2 periods. Organ suppression is related to cell cycle arrest, because Histone H4 is not expressed in stamens in female flowers or in pistils in male flowers in *Phoenix dactylifera* (Daher et al., 2010).

Developmental suppression is caused by cell cycle arrest, because Cyclin B is not expressed in the stamen primordia in the female flowers in *Z. mays.* The terminal deoxynucleotidyl transferase dUTP nick end labeling (TUNEL) signal, which detects cell death, is observed in the pistil primordia of male flowers of *Z. mays* (Kim et al., 2007). Specific TUNEL signals and chromatin condensation are detected in the stamen

primordia of the female flowers at Stage 7 for *C. sativus* (Hao et al., 2003). However, TUNEL signals and chromatin condensation are not detected in the pistils of the male flowers of *C. sativus* (Bai et al., 2004). Cell death is detected only in the pistil primordia of the male flowers of *Z. mays* using a TUNEL assay (Kim et al., 2007). Cell death is detected only in the stamen primordia in *C. sativus* female flowers (Hao et al., 2003). The suppression mechanisms of pistil primordia in male flowers and in the stamen primordia in female flowers differ in diclinous plants.

Cell death in tissues of dioecious plants is detected by the TUNEL assay, but practical examples of the TUNEL assay in dioecious plants do not exist. However, it is well known that programmed cell death occurs in tapetal cells in plants. The TUNEL assay is often used on tissue sections to detect cell death in tapetal cells (Li et al., 2006). The programmed cell death of tapetal cells is characterized by a gradual decrease in cytoplasm structure. Cytoplasmic reduction, fragmentation of DNA, vacuolar explosion, and elongation of the endoplasmic reticulum have been observed as tapetal cells in *Lobiva raushii* and *Tillandsia albida* collapse (Papini et al., 1999). The programmed cell death of the tapetal cell occurs with the postmeiotic development process (Sanders et al., 1999).

The bisexual form was observed in the male and the female flowers of *S.*

latifolia in Stages 1–6 (Grant et al., 1994). The pistil developed in the female flower after Stage 7, and the stamen was suppressed. Then, the stamen developed and the pistil was suppressed in the male flower. *M. violaceum* has recently been differentiated into three species due to host specificity, one being renamed *M. lychnidis-dioicae* (Denchev et al., 2009). Male flowers infected with *M. lychnidis-dioicae* formed a smut spore instead of pollen in the anthers. The female flowers infected with *M. lychnidis-dioicae* formed stamens, which are typically not formed in female flowers, and the stamens formed smut spores instead of pollen in the anthers (Uchida et al., 2003).

In this study, I investigated whether cell death or cell cycle arrest was related to flower organ formation in *S. latifolia* (Fig. 1-1). I was able to identify a clear relationship between the stamen extension caused by *M. lychnidis-dioicae* and cell death or cell cycle arrest in flower organs, as suppression of stamens in the female flowers of *S. latifolia* was eliminated by infection with *M. lychnidis-dioicae*. As a result, it became clear that cell death and cell cycle arrest occur in the pistils of male flowers and in the stamens of female flowers. Cell death and cell cycle arrest were not observed in the stamens of female flowers infected with *M. lychnidis-dioicae*.

MATERIALS AND METHODS

Plant materials and plant growth conditions

S. latifolia seeds of inbred lines were stored (K-line) in our laboratory. The K-line was propagated for 17 generations of inbreeding to obtain a genetically homogeneous population. I also used asexual mutants, which were obtained from crossing an asexual mutant (ESS1) and an inbred line (K-line). Plants were grown from vernalized seeds in pots in a regulated chamber at 23℃, with 16-h light/8-h dark cycles.

M. lychnidis-dioicae inoculation

A1 and A2 sporidial were cultured on potato dextrose agar (BD difco) at 23℃ for 5 d and suspended at 2 ×106 cells/mL in distilled water. Equal concentrations of A1 and A2 sporidial mixtures used throughout the inoculations. The inoculation treatments were performed on 10-d-old seedlings of *S. latifolia* on 0.8% agar plates. The base of each 10-d-old seedling was injected with 2 μL of the mixture. Inoculation was repeated after 3 d. Three weeks after the inoculation, I transferred seedlings to soil in pots and grew them in a regulated chamber at 23℃, with a 16-h light/8-h dark cycle.

In situ hybridization

Total RNA (100 ng) was reverse-transcribed into cDNA using a first-stand cDNA synthesis kit (GE Healthcare Biosciences, Buckinghamshire, UK). The probes used were *SlCycA1* and *SlH4*, with the *SlCycA1* specific-primer (*SlCycA1F*, 5'-GGAACGCTACTTTGCGGCAT-3' and *SlCycA1R*, 5'-CTACAGTCTCAGTACATGGC-3') and SlH4 specific-primer (*SlH4F2*, 5'-AGGAAAAAAGAAGACCAAAC-3' and *SlH4R2*, 5'-AAACCCGAAACCAAAACGAA-3'). The amplified insert was used to produce digoxigenin (DIG)-labeled sense and antisense RNA probes, using a DIG RNA Labeling Kit SP6/T7 (Roche Applied Science, Indianapolis, USA). Flower buds were immediately fixed in FAA solution (3.7% [v/v] formaldehyde, 50% [v/v] ethanol, and 5% [v/v] acetic acid) at 4℃. The fixed buds were dehydrated in an ascending ethanol series (25, 50, 75, and 100%; each step for 20 min at 4℃) and stored overnight in 100% ethanol. The samples were embedded in HISTOSEC (MERK). The 8-μm sections were cut with a microtome and mounted on slides at 37℃ overnight. *In situ* hybridization was performed as described by Kazama et al. (2005).

TdT-mediated dUTP nick end labeling (TUNEL) assay

Flower buds were immediately fixed in FAA solution (3.7% [v/v]

formaldehyde, 50% [v/v] ethanol, and 5% [v/v] acetic acid) at 4℃. Anthers were immediately double fixed overnight in 4% glutaraldehyde in 0.1 M phosphate buffer (pH 7.2) at 4℃ and post-fixed for 4 h in 2% osmium tetraoxide in distilled water. After being washed in 0.1 M phosphate buffer (pH 7.2), the fixed flowers were dehydrated in an ethanol series (30, 50, 70, 80, 90, 95, and 100%, each step for 15 min at room temperature) and stored overnight in 100% ethanol at 4℃. The ethanol was replaced with xylen and embedded in paraffin. Flowers embedded in paraffin were cut into 10-μm sections using a microtome (RV-240, Yamato, Japan). Cutting sections were deparaffinized in xylen and rehydrated in an ethanol series (100, 95, 90, 80, 70, 50, and 30%, each step for 10 min at room temperature).

In situ nick end labeling of nuclear DNA fragmentation was performed in a humid chamber for 1 h in the dark at 37°C with an *In Situ* Cell Death Detection Kit (Roche) in flower buds and with a Click-iT TUNEL Alexa Fluor 647 Imaging Assay for microscopy and HCS in anthers. Samples were analyzed under a fluorescence microscope (LeicaCTR6000, Leica Microsystems, Heidelberg, Germany). The fluorescent filter was set to view the green fluorescence of fluoresce at 527 ± 30 nm, the infrared fluorescence of Alexa Fluor 647 at 700±70 nm, and the blue fluorescence of DAPI at 470 ± 40 nm.

Transmission electron microscopy

Flower buds were dissected with fine forceps, placed in 1-Hexadecene, and frozen in a high-pressure freezing machine (HPM010, BAL-TEC) that was cooled with liquid nitrogen (−196℃). The samples were immediately transferred to 2% OsO_4 in dry acetone at −0℃ and incubated at −80℃ for 100 h. The samples were then gradually warmed from −80℃ to 0℃ over 5 h, held for 1 h at 0℃, warmed again from 0℃ to 23℃ over 1 h, and incubated for 1 h at 23℃ (Leica EM AFS, Leica Microsystems). The samples were washed three times with dry acetone at room temperature, infiltrated with increasing concentrations of Spurr's resin (Kushida, 1980) in dry acetone, and finally infiltrated with Suppr's resin. Ultra-thin sections (50 nm) were cut with a diamond knife (DIATOME Ltd) and mounted onto Formvar-coated copper grids. The sections were stained with 3% uranyl acetate for 2 h at room temperature and examined using an electron microscope (H-7600, Hitachi co. Tokyo, Japan) at 100 kV.

RESULTS

Cell division at organ extension and mature stages

Differences were not observed between males and females at Stages 3–4 (Fig.

1-2a–d), which are early developmental stages. However, developmental suppression was observed in the pistils in male flowers and in the stamens in female flowers from Stages 7–8 (Fig. 1-2e–h), which are organ extension stages, to Stages 10–11 (Fig. 1-2i–p), which are mature stages. To detect cell cycle arrest in these suppression organs, I investigated the distribution of dividing cells using double dyeing *in situ* hybridization (ISH), which uses SlCycA1, cyclin of *S. latifolia*, SlH4, and Histone H4 of *S. latifolia* in the pistils and stamens of the wild-type (WT) males and females in early developmental stages (Stages 3–4), organ extension stages (Stages 7–8), and mature stages (Stages 10–11). I considered the cells, which detect the signals of both histone and cyclin genes, to be dividing during the S period.

Both signals were detected in the stamen and pistil primordia of the WT female flowers in early developmental stages (Fig. 1-2 a). Both signals were detected in the developing pistils (dp) of the WT female flowers in the organ extension stages (Stages 7–8; Fig. 1-2 e). Many signals were detected in the dg, especially the ovaries (o) and ovary walls (ow), in the WT female flowers at the mature stages (Stages 10–11; Fig. 1-2 i, m). Neither signal was detected in the suppressed stamens (ss) of the WT female flowers at the mature stages (Stages 10–11; Fig. 1-2 i, m). Therefore, it was revealed that cell division was arrested in the ss of the WT female flowers at the mature stages

(Stages 10–11; Fig. 1-2 i, m).

Differences were not observed in these stages in the male flowers infected with *M. lychnidis-dioicae* (Fig. 1-2 d, h, l, p). Signals were detected in the developmental stamens (ds) of female flowers infected with *M. lychnidis-dioicae* in the organ extension stages (Stages 7–8; Fig. 1-2 f) as well as the WT male flowers (Fig. 1-2 g) and male flowers infected with *M. lychnidis-dioicae* (Fig. 1-2 h).

Signals were detected in the ds in female flowers infected with *M. lychnidis-dioicae* during the mature stages (Stages 10–11), but there were fewer signals than in the WT male flowers (Fig. 1-2 j, k, n, o). The cell division activity in the stamens of the female flowers infected with *M. lychnidis-dioicae* was lower than that in the WT male flowers.

Developmental suppression of organ and cell death

I performed the TUNEL assay in WT female and male flowers and in male and female flowers infected with *M. lychnidis-dioicae* during the early developmental stages (Stages 3–4; Fig. 1-3 a–d), organ extension stages (Stages 7–8; Fig. 1-3 e–h), and mature stages (Stages 10–11; Fig. 1-3 i–p). The TUNEL assay is used to detect double-strand breaks. I visualized the florescent TUNEL signals using fluorescein

isothiocyanate (FITC). 4',6-diamidino-2-phenylindole (DAPI) was used as a red nuclear marker, the TUNEL signal was green, and the combination of TUNEL and DAPI signals was yellow.

TUNEL signals were not detected in the WT female or male flowers during the early developmental (Stages 3–4) or organ extension (Stages 7–8; Fig. 1-3 a, h) stages. TUNEL signals were detected in the ss of the WT female flowers during the mature stages (Stages 10–11; Fig. 1-3 i, m). Cell death did not occur in the pistils or stamens of female flowers infected with *M. lychnidis-dioicae*, as TUNEL signals were not detected (Fig. 1-3 j, n). However, TUNEL signals were detected in the suppressed pistils (sp) in the WT male flowers (Fig. 1-3 k, o). TUNEL signals were observed over the base from the center of the sp but these signals were not confirmed because they were weak, with low magnification. TUNEL signals were detected in the males infected with *M. lychnidis-dioicae*, as well as in the sp of the WT male flowers (Fig. 1-3 l, p). These results showed that cell death occurred in the suppressed pistils of WT males and in the male flowers infected with *M. lychnidis-dioicae* at maturity, as well as in the suppressed stamens of WT females at maturity (Stages 10–11).

***Cell death in the pollen sac and* M. lychnidis-dioicae**

In addition to the stamen and pistil primordia, which reflected cell death in the plant, TUNEL signals were detected in tapetal cells in the anthers (Fig. 1-3 q, r, s, t). Anthers of *S. latifolia* infected with *M. lychnidis-dioicae* formed smut spores instead of pollen. I studied the cell death of the pollen mother cells and how they were removed when *M. lychnidis-dioicae* formed spores. First, I applied the anther development stages, which Sanders et al. defined in *Arabidopsis thaliana*, to *S. latifolia* and indicated anther developmental stages of *S. latifolia* with a Roman numeral to distinguish them from flower developmental stages (Figs. 1-5, 1-6; Sanders et al., 1999). I performed the TUNEL assay to investigate whether I could distinguish the cell death of the pollen mother from that of the tapetal cells in male flowers infected with *M. lychnidis-dioicae* during Stages V–VIII (Figs. 1-4, 1-5).

I used high magnification to observe the pollen mother and tapetal cells in the anthers. I could not detect programmed cell death in tapetal cells using a FITC-labeled TUNEL assay because tapetal cells strongly auto-fluoresce in the 520 nm range (Fig. 1-3 r, s, t). Therefore, I used Alexa 647 to observe anthers in an infrared region with the least auto-fluorescence. The nucleus was stained with DAPI, as indicated by blue, whereas TUNEL-positive nuclei were indicated by magenta and white merged with blue and magenta.

TUNEL signals were not detected in the WT male flowers at Stage V (Fig. 1-5 a-1–a-6). At Stage VI, the TUNEL signal was detected in the tapetal and pollen mother cells during meiosis (Fig. 1-4 b-1–b-6). TUNEL signals were detected with tapetal cells only in Stages VII and VIII (Fig. 1-4 c-1–c-6, d-1–d-6). TUNEL signals were detected in parts of just a few tapetal cells during Stage IX (Fig. 1-4 e-1–e-6).

TUNEL signals were detected with tapetal cells only in the male flowers infected with *M. lychnidis-dioicae* at Stage V (Fig. 1-5 a-1–a-6). During Stages VI–VIII, the pollen mother cell also collapsed, but the liquid-state-formed TUNEL signals was detected only in tapetal cells (Fig. 1-5 b-1–b-6, c-1–c-6, d-1–d-6). The TUNEL signals were only detected with the tapetal cells at Stage IX (Fig. 1-5 e-1–e-6). The TUNEL signals were detected only in the tapetal cells in pollen sacs of male flowers infected with *M. lychnidis-dioicae*. The collapse of the pollen mother in pollen sacs of male flowers infected with *M. lychnidis-dioicae* was due to the necrosis-like cell death without the TUNEL signal.

Observation of the collapse of tapetal cells using transmission electron microscopy

I observed pollen sacs in Stages VI and VII using transmission electron microscopy. The nebula-formed TUNEL signals were observed in the tapetal cells of the

male flowers infected with *M. lychnidis-dioicae* but not in the tapetal cells in WT male flowers (Fig. 1-5). As a result, I discovered that the collapse of the membranes and cell walls of the tapetal cells in the male flowers infected with *M. lychnidis-dioicae* was caused by *M. lychnidis-dioicae* infection, and the contents of the cells were eluted (Fig. 1-6 a, b). The tapetal cells, in which I detected TUNEL signals in the male flowers infected with *M. lychnidis-dioicae*, were impaired at the nuclear membranes and formed numerous vacuoles at Stage VI (Fig. 1-6 a). The cell then completely collapsed in a high electron density karyoplasm, and the vacuole was observed (Fig. 1-6 b). The high electron density karyoplasm was in the same area as the tapetal cells and the area of the liquid-state-formed TUNEL signal (Figs. 1-5, 1-6). I also only detected the TUNEL signal in tapetal cells in the pollen sacs in the male flowers infected with *M. lychnidis-dioicae*, as TUNEL signals were not detected in the collapse of pollen mother cells caused by *M. lychnidis-dioicae*.

DISCUSSION

Usefulness of the TUNEL assay for observing the infrared region in the plant

The TUNEL assay is effective for detecting cell death in animals (Grasl-Kraupp et al. 1995). There are fewer examples of applying the TUNEL assay to

plants compared with animals. This difference is attributable to strong auto-fluorescence in plants. I performed the TUNEL assay in the infrared region, which has the weakest auto-fluorescence in tapetal tissues. The auto-fluorescence of tapetal tissue was very strong near 520 nm (Figs. 1-4, 1-5). The auto-fluorescence of chlorophyll consisted of red (near 685–690 nm) and infrared (near 730–740 nm) regions (Buschmann 2007). However, chloroplasts do not exist in stamens and pistils. Therefore, I could avoid auto-fluorescence by using the infrared region (near 730–740 nm).

Drs. Hao and Bai performed the TUNEL assay in a light field (Hao et al., 2003; Bai et al., 2004), and Dr. Kim performed the TUNEL assay as fluorescent labeling with FITC; this approach detected strong auto-fluorescence near 520 nm (Kim et al., 2007). However, it was difficult to detect a clear signal. I was able to get a clear signal in the tapetal cells, as the TUNEL assay was effective in the infrared region in flower organs (Figs. 1-4, 1-5).

The TUNEL signal was detected in pollen mother and tapetal cells during meiosis in Stage 6 (Fig. 1-5 c-4, c-5, c-6). Double-strand breaks, indicating recombination during meiosis, were detected. I was able to detect double-stranded breaks, such as recombination during meiosis, using high resolution, as auto-fluorescence was eliminated and observation in the infrared region was facilitated.

Cell death and cell cycle arrest in the flower organ

Stamens were completely suppressed in the mature female flowers of *S. latifolia*. Pistils of the mature male flowers remained as filament-formed rudimentary organs (Grant et al., 1994). Cell cycle arrest in the pistils of male flowers was less severe than cell cycle arrest in the stamens of female flowers (Fig. 1-2 m–p). TUNEL signals were detected only in a few cells of the pistils (Fig. 1-3 m–p). Therefore, I think that the pistils of the male flowers remain as rudimentary organs due to the weak developmental suppression of their pistils.

Development of the female flower stamens was suppressed by cell death, and the pistils of the male flowers were suppressed by arresting the cell division in *Z. mays* (Kim et al., 2007). Cell death was not observed in the pistils of the male flowers in *C. sativus*. Cell death, accompanied by the TUNEL signal, was observed in the stamens of female flowers (Hao et al., 2003; Bai et al., 2004). Developmental suppression of *C. sativus* and *Z. mays* was related to either cell cycle arrest or death. I identified cell cycle arrest by ISH using Cyclin B and Histone H4 probes, similar to the technique of Matsunaga et al. (2004) (Fig. 1-2). I determined cell death using the TUNEL assay (Fig. 3). When the pistil of the male flower and the stamen of the female flower were

suppressed in *S. latifolia*, cell death and cell cycle arrest were detected. On the other hand, when the pistil of the male flower and the stamen of the female flower were developed in *S. latifolia*, cell division was detected (Figs. 1-3 i, m, l, p; 4 i, m, l, p). Therefore, I suggest that the function of suppressing flower development may not be specialized between the male and female in *S. latifoli*a because of differences between dioecious plants, such as *S. latifolia*, and diclinous plants, such as *C. sativus* and *Z. mays*, or because of the sexual differentiation of *S. latifolia*. Therefore, it was concluded that both cell cycle arrest and death, reflecting developmental suppression, were present in male and female flowers in *S. latifoia*.

Lytic cell death in the tapetal cell

Tapetal cells exist in the innermost four layers that form anthers, and these include the epidermis, endothecium, middle layer, and tapetum. The tapetal cells directly touch the gametophyte, which become pollen and play an important role in development from microspore to pollen (Pacini et al., 1985). The tapetal cell, as a secretion cell layer, provides nourishment for a microspore released from a pollen tetrad until pollen development (Goldberg et al., 1993). The cytoplasm of the tapetal cell collapses in the late stage of pollen development. It is thought that this process of the

collapse in the tapetal cell is related to programmed cell death in many plants (Papini et al., 1999; Wu and Cheun 2000). Programmed cell death of the tapetal cells is characterized by a graded decrease in cytoplasm structure. Cytoplasmic reductions, fragmentation of DNA, a vacuolar explosion, and elongation of the endoplasmic reticulum have been observed during collapse in the tapetal cells in *Lobiva raushii* and *Tillandsia albida* (Papini et al., 1999). Tapetal cell collapse occurs at the same time as the postmeiotic developmental process of pollen mother cells (Sanders et al., 1999). Malfunction of the tapetal cells triggers male sterility (Sorensen et al., 2002; Yang et al., 2003).

Tapetal cells include amoeba and secretion types, and most of the angiosperm are of the secretion type of tapetal cells. The thickness of the secretion tapetal cell walls in *A. thaliana* is reduced before pollen mother cells perform meiosis, and the pollen mother cells simultaneously thin (Matsuo et al., 2013).

Lytic cell death was observed when the cell walls of males of *S. latifolia* infected with *M. lychnidis-dioicae* thinned before meiosis (Fig. 1-6 a, b). Cell death seen in the tapetal cells in the males infected with *M. lychnidis-dioicae* caused programmed cell death, with the fragmentation of DNA as expected. However, it is thought that the nucleus and its contents is eluted from tapetal cells, because collapse of

the cell walls and membranes is caused by *M. lychnidis-dioicae*.

M. lychnidis-dioicae and cell death

The TUNEL signal is detected in the tapetal cells with pollen development (Fig. 4). Tapetal cells collapse to supply nutrition and sporopollenin, which are components of the pollen wall (Goldberg et al., 1993). Male sterility, which occurs when pollen is not formed, is caused by collapsed tapetal cells. Pollen mother cells are killed and eliminated in the anther of males infected with *M. lychnidis-dioicae* (Uchida et al., 2003). However, cell death with TUNEL signals was not observed with the tapetal cells in the pollen mother cell (Fig. 1-5). These TUNEL signals were in a liquid-state, unlike normal TUNEL signals. I hypothesized that the fragmented nucleus with the TUNEL signal was detected in pollen sacs, caused by tapetal cell collapse, and eluted to pollen sacs due to the cell death of the tapetal cells, which had occurred earlier as a result of *M. lychnidis-dioicae*. In other words, *M. lychnidis-dioicae* caused cell death, but it could not inhibit cell death from the anthers. *M. lychnidis-dioicae* does not inhibit cell death and affects cell cycle and expression of B or C function genes, because it promotes formation of stamens in female flowers (Figs. 1-2 b, f, j, n; 3 b, f, j, n), and *M. lychnidis-dioicae* did not control cell death (Fig. 1-6). *M. lychnidis-dioicae* changed the

expression of upper genes, but it could not directly control cell death due to expression of *SLM2*, which is a homolog of *PISTILLATA* of the B function gene in *A. thaliana*, which is induced when *M. lychnidis-dioicae* infects male flowers (Kazama et al., 2005).

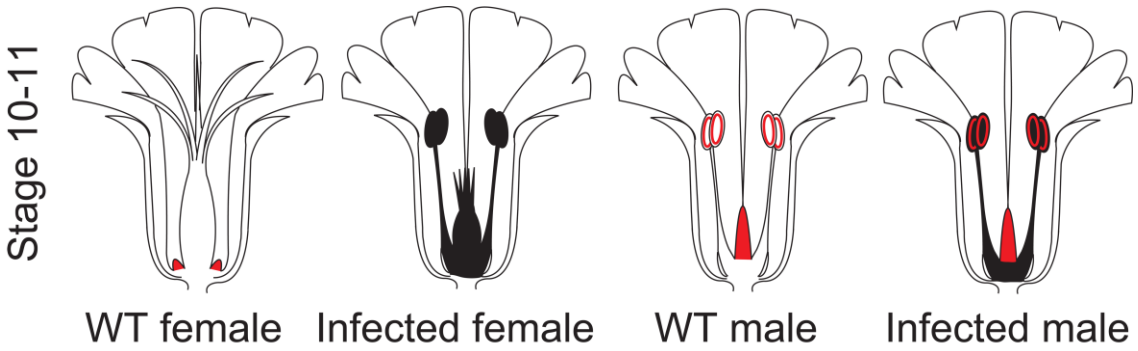

Fig. 1-1 Schema of areas predicted to exhibit cell death and cell cycle arrest in the flower organs of a wild-type (WT) female, an infected female, a WT male, and an infected male. I hypothesized that cell death and/or cell cycle arrest can be detected in the areas shown in red. The black area indicates that the flower was infected with smut fungus.

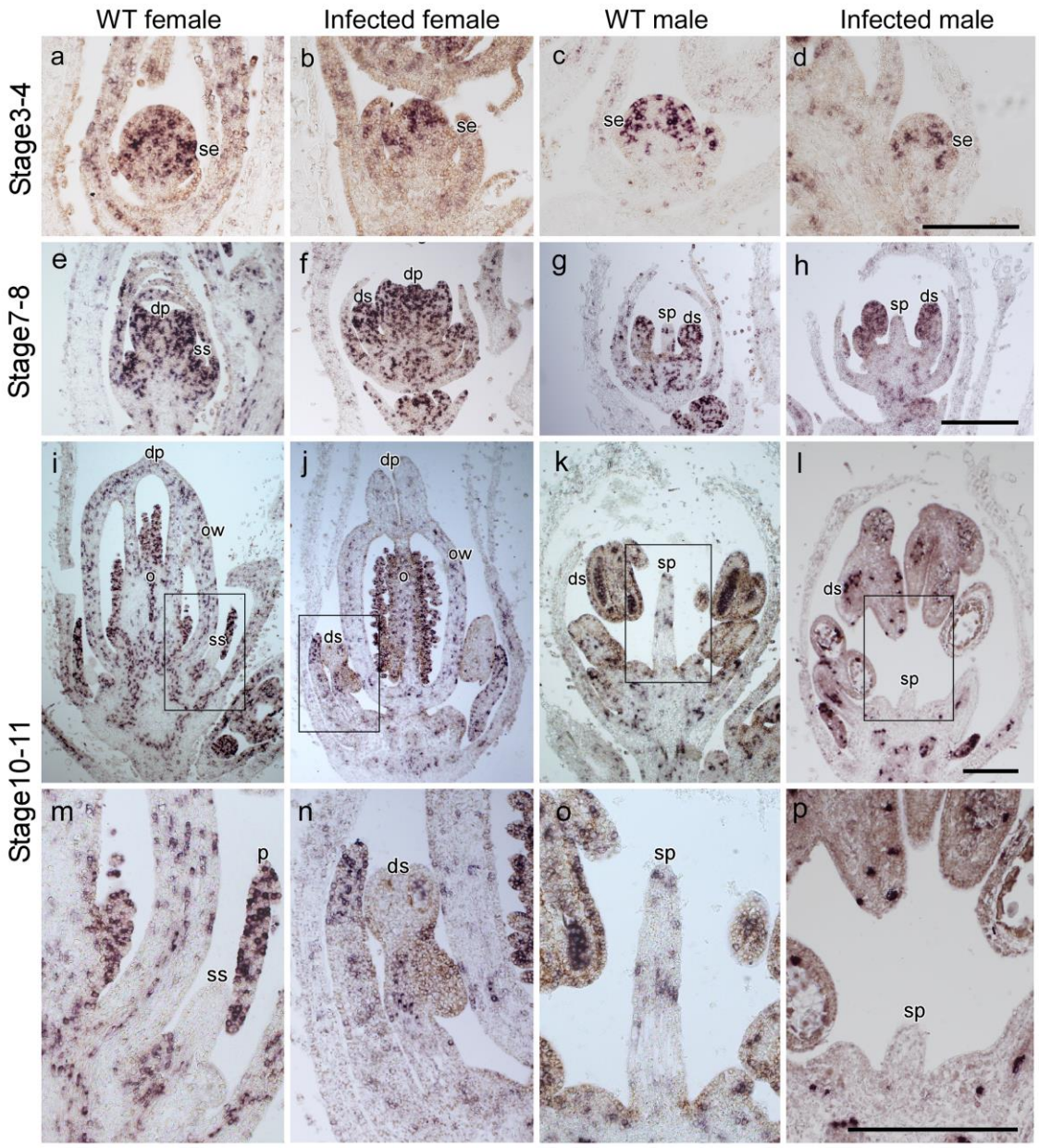

Fig. 1-2 *In situ* hybridization using Cyclin B and Histone H4 probes in Stages 3–4, 7–8, and 10–11 of WT males, WT females, infected males, and infected females. Signals were detected in Stages 3–4 (**a–d**) and 7–8 (**e–h**) of each flower bud meristem (**a–h**). Signals were detected in the suppressed stamen in Stages 10–11 of WT females (**i, m**). Signals were not detected in the suppressed pistil in Stages 10–11 of WT males or

infected males (**k, l, o, p**). However, signals were detected in the developed filament in Stages 10–11 of the infected females, but signals were not detected in the anther (**j, n**). **a** Female flowers at Stages 3–4, **b** Infected female flowers at Stages 3–4, **c** Male flowers at Stages 3–4, **d** Infected male flowers at Stages 3–4, **e** Female flowers at Stages 7–8, **f** Infected female flowers at Stages 7–8 , **g** Male flowers at Stages 7–8 , **h** Infected male flowers at Stages 7–8 , **i**, **m** Female flowers at Stages 10–11, **j**, **n** Infected female flowers at Stages 10–11, **k**, **o** Male flowers at Stages 10–11, **l**, **p** Infected male flowers at Stages 10–11. Squares indicate high-magnification areas. Developed stamen (**ds**), Developed pistil (**dp**), Ovule (**o**), Ovary wall (**ow**), Sepal (**se**), Suppressed stamen (**ss**), Suppressed pistil **(sp)**, and Petal (**p**). Bar = 100 μm for a to p.

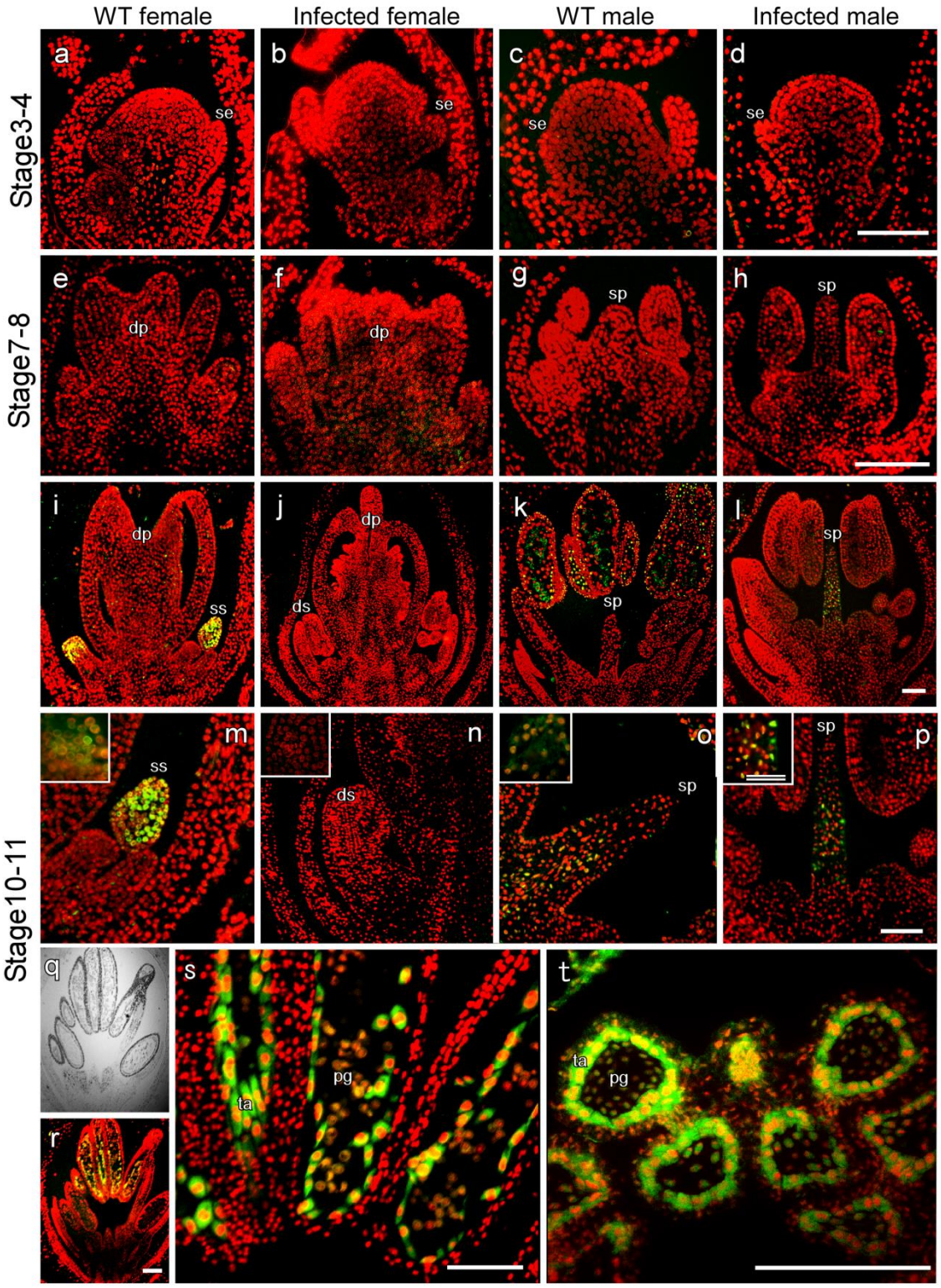

Fig. 1-3 Terminal deoxynucleotidyl transferase dUTP nick end labeling (TUNEL) assay in Stages 3–4, 7–8, and 10–11, and pollen sacs of WT males, WT females, infected

males, and infected females. Signals were not detected in Stages 3–4 (**a–d**) or 7–8 (**e–h**) of each flower bud meristem. Nuclei are indicated by red fluorescence, while TUNEL-positive nuclei are indicated by green fluorescence (**a–h**). Signals were detected in the suppressed stamen in Stages 10–11 of WT females (**i**, **m**). Signals were detected in the suppressed pistil in Stages 10–11 of WT males and the infected males (**k**, **l**, **o**, **p**). However, signals were not detected in the developed stamens in Stages 10–11 of infected females. A female flower at Stages 3–4, **b** An infected female flower at Stages 3–4, **c** A male flower at Stages 3–4, **d** An infected male flower at Stages 3–4, **e** A female flower at Stages 7–8, **f** An infected female flower at Stages 7–8, **g** A male flower at Stages 7–8, **h** An infected male flower at Stages 7–8, **i**, **m** A female flower at Stages 10–11, **j**, **n** An infected female flower at Stages 10–11, **k**, **o** A male flower at Stages 10–11, **l**, **p** An infected male flower at Stages 10–11, **q** Bright field images of a WT male at Stages 10–11 , **r** Fluorescent image of a WT male at Stages 10–11. **s** high magnification of anthers from **r**. **t** Pollen sacs. Squares indicate high-magnification areas. Developed stamen (**ds**), Developed pistil (**dp**), Pollen grain (**pg**), Suppressed stamen (**st**), Suppressed pistil **(sp)**, Sepal (**se**) and Tapetal cell (**ta**). Bar = 100 μm for a to t. Double bar = 50 μm for m to p.

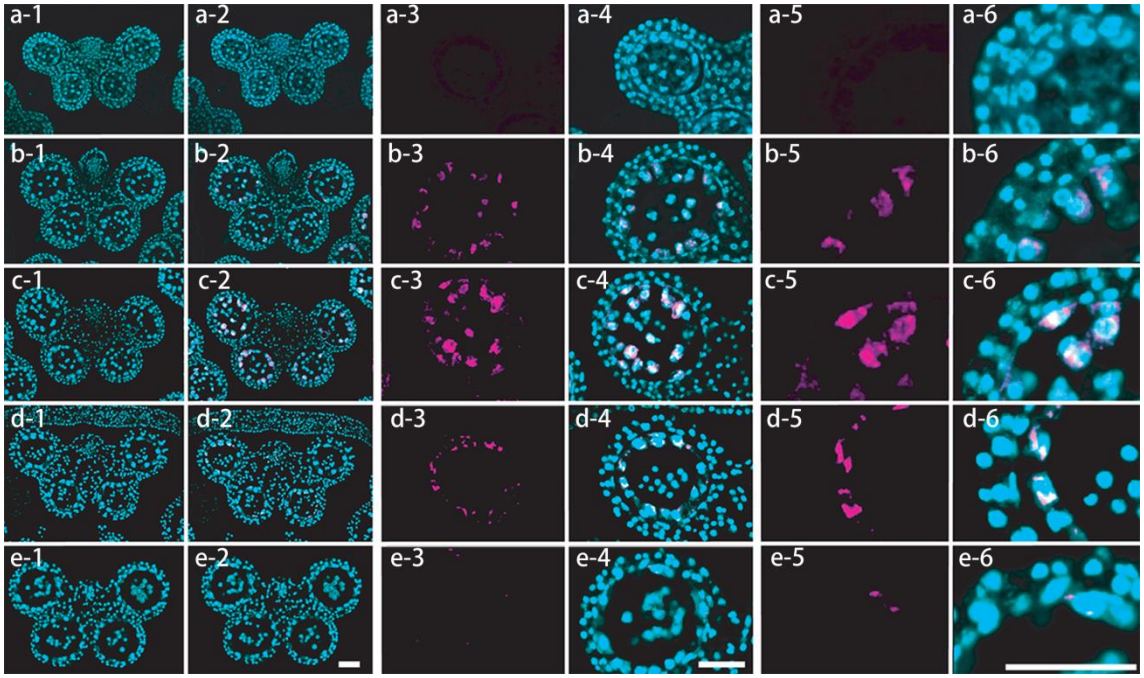

Fig. 1-4 High-resolution TUNEL assay in WT anthers. The anthers of the five developmental stages in WT males were compared for nuclear DNA fragmentation using a TUNEL assay. Nuclei were stained with 4',6-diamidino-2-phenylindole (DAPI), as indicated by blue, whereas TUNEL-positive nuclei are indicated by magenta and appear white when the blue and magenta areas are merged. (**a-1~a-6**) WT males at Stage 5, (**b-1~b-6**) WT males at Stage 6, (**c-1~c-6**) WT males at Stage 7, (**d-1~d-6**) WT males at Stage 8, (**e-1~e-6**) WT males at Stage 9. Bars = 50 μm for a-1 to e-6.

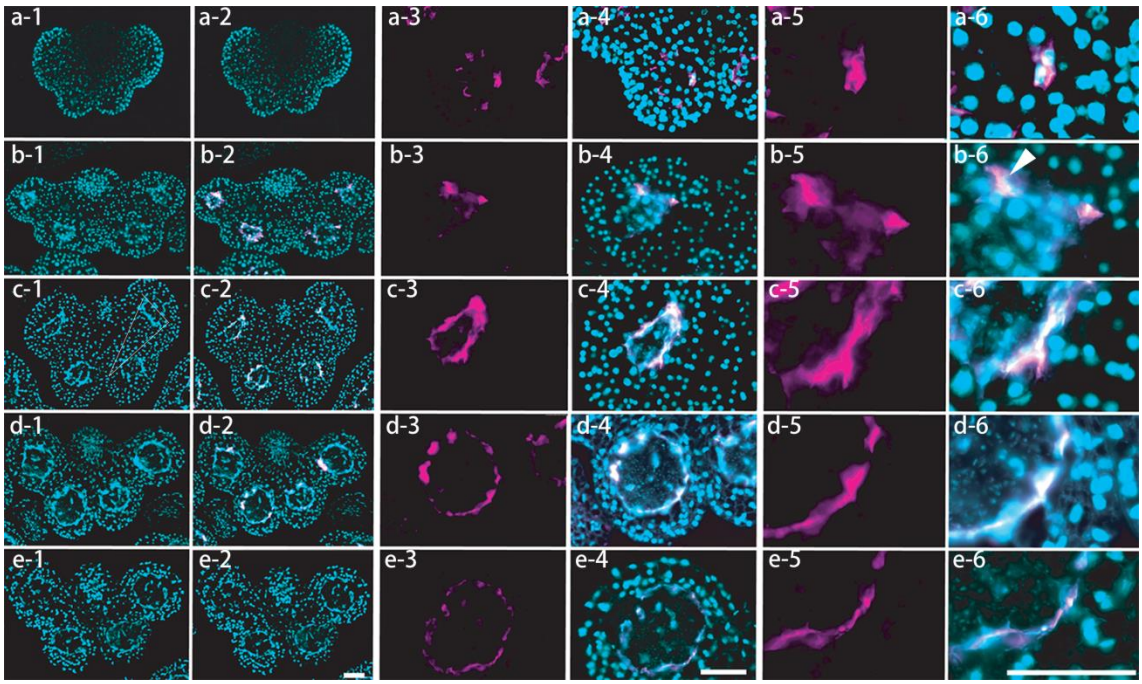

Fig. 1-5 High-resolution TUNEL assay in male anthers infected with *M. lychnidis-dioicae.* The anthers of the five developmental stages in male anthers infected with *M. lychnidis-dioicae* were compared for nuclear DNA fragmentation using the TUNEL assay. Nuclei were stained with DAPI, as indicated by blue, whereas TUNEL-positive nuclei were indicated by magenta and appear white when the blue and magenta areas are merged. **a-1~a-6** An infected male at Stage 5, **b-1~b-6** An infected male at Stage 6, **c-1~c-6** An infected male at Stage 7, **d-1~d-6** An infected male at Stage 8, **e-1~e-6** An infected male at Stage 9. Arrowhead indicates a high electron density karyoplasm, likely the same structure indicated in Fig. 6. Bars = 50 μm for a-1 to e-6.

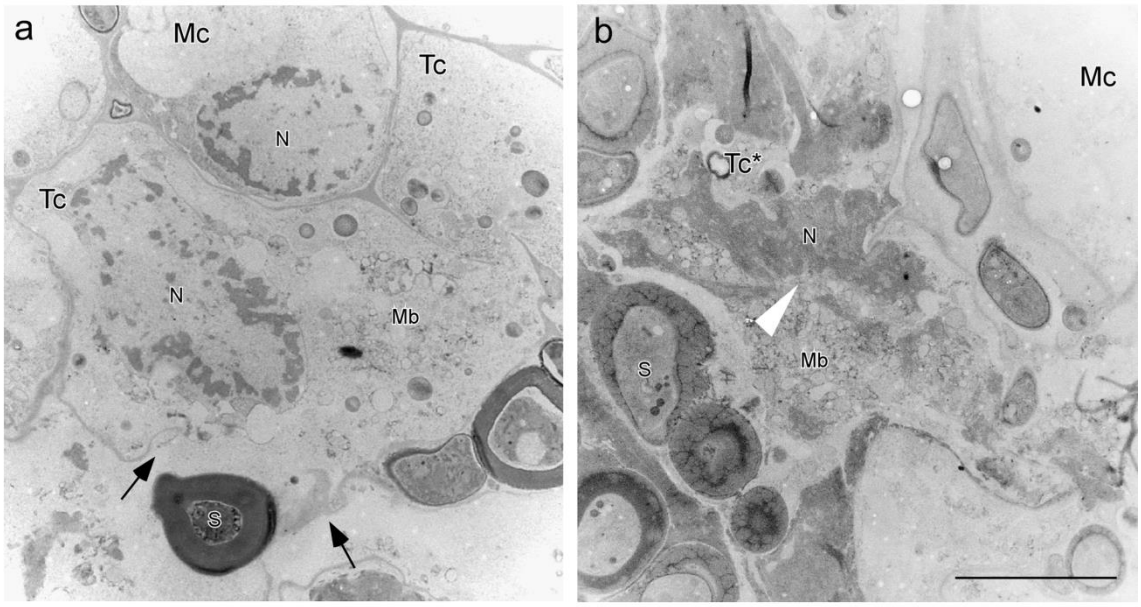

Fig. 1-6 Transmission electron micrographs of tapetal cells in infected males. Tapetal cells lead to abnormal disintegration caused by *M. lychnidis-dioicae* infection. **a** Tapetal cells in an infected male at Stage 6, **b** Disintegrated tapetal cells in an infected male at Stage 7. Arrows indicate a disrupted cell wall. Arrowhead indicate a high-electron-density karyoplasm, **Mc** Middle layer cell, **Mb** Multivesicular body, **N** Nucleus, **S** Spore, **Tc** Tapetal cells, **Tc*** Disintegrated tapetal cells. Bar = 2 μm for a and b.

CHAPTER II

An asexual flower of *Silene latifolia* and *Microbotryum lychnidis-dioicae* promoting its sexual-organ development

本博士論文中、2 章（pp.35-64）の部分は、*Journal of Plant Research* に掲載等の形で刊行される予定であるため、学位授与日から 5 年間インターネットでの公表をすることができません。

CHAPTER III

Three-dimensional ultrastructural study of the anther of *Silene latifolia* infected with *Microbotryum lychnidis-dioicae*

本博士論文中、3 章（pp.65-89）の部分は *PLOS ONE* 掲載等の形で刊行される予定であるため、学位授与日から 5 年間インターネットでの公表をすることができません。

CONCLUSIONS

In this study, I tried to reveal relation of *S. latifolia* and *M. lychnidis-dioicae*. I demonstrated the following three points concerning the study of the plant physiology and plant pathology:

1. I investigated the role of cell cycle arrest and cell death in the developmental suppression of male and female flower organs and investigated the relationship between *M. lychnidis-dioicae* infection and suppression of the male and female flower organs. In addition, it is known that TUNEL-positive cell death occurs in the tapetal cells of plants. I investigated whether TUNEL-positive cell death occurred in other anther cells, including the endothecium, the middle layer, and pollen mother cells, after *M. lychnidis-dioicae* infection. The results of this study demonstrate that cell death and cell cycle arrest occur in the pistil of the male flower and the stamen of the female flower. Cell death and cell cycle arrest were not seen in the stamen of the female flower infected with *M. lychnidis-dioicae***.**

2. The purpose and conclusion of the chapter 2 was as follows : 1. What happens when *M. lychnidis-dioicae* infects asexual mutants with parietal deletions in the Y chromosome? In asexual mutants, development of the stamen and gynoecium is suppressed. If suppression of stamen and gynoecium development functions through the same mechanism, then suppression of gynoecium development should be released when suppression of stamen

development is released by *M. lychnidis-dioicae* infection. 2. What differences exist in stamens between the infected asexual mutant, the infected male, and the infected female? I infer that I are able to search for genes related to anther development, which should exist in the deleted region of the Y chromosome, by comparing pollen sacs of stamens in the infected male, infected female, and infected asexual mutant. The results of this study demonstrate that developmental suppression of the stamen was released by *M. lychnidis-dioicae*, but that of gynoecium development was not released. In addition, I found that differentiation of the archesporial cells did not occur in the anther of the infected female, whereas the tapetal cells were abnormally formed in the anther of the asexual mutant. These results suggest that the Y chromosome of the asexual mutant has genes related to the differentiation of archesporial cells, but none related to maturation of the tapetal cells.

3. *M. lychnidis-dioicae* hyphae are present in the pollen sac at flower developmental stage 8. *M. lychnidis-dioicae* initiation teliospore was observed surrounding dead or dying pollen mother cells flower developmental stage 9. When *M. lychnidis-dioicae* invasion occurs in the anther has been unclear; therefore it is important to investigate not only whether hyphae exist when the apical meristem tissue differentiates into flowers and anthers, but also whether hyphae exist when stamen filaments are formed. I used Modified Grocott's methenamine silver stain and lectin staining using a fluorescently labeled lectin, WGA to search for *M. lychnidis-dioicae* in flower tissues. *M. lychnidis-dioicae* invaded the anther at

anther developmental stage III, and the hyphae invaded the anther through the stamen filament. Moreover, I showed that *M. lychnidis-dioicae* branched out from connective, adhering to the stamen filament, toward the center of the pollen sacs, and the host cells collapsed near the hyphae with thick cell walls and teliospores. These results support the hypothesis that the presence of teliospores induced the collapse of the cell wall and degeneration of cells because these phenomena were seen only around hyphae with thick cell walls.

REFERENCES

Ainsworth C (2000) Boys and girls come out to play: The molecular biology of dioecious plants. Ann Bot 86:211–221.

Alexander HM, Antonovics J (1988) Disease spread and population dynamics of anther-smut infection of *Silene alba* caused by the fungus *Ustilago violacea*. J Ecol 76:91.

Alexander HM, Maltby A (1990) Anther-smut infection of *Silene alba* caused by *Ustilago violacea*: factors determining fungal reproduction. Oecologia 84:249–253.

Bai S-L, Peng Y-B, Cui J-X, Gu H-T, Xu L-Y, Li Y-Q, et al (2004) Developmental analyses reveal early arrests of the spore-bearing parts of reproductive organs in unisexual flowers of cucumber (*Cucumis sativus* L.). Planta 220:230–40.

Baker HG (1947) Infection of species of *Melandrium* by *Ustilago violacea* (Pers.) Fuckel and the transmission of the resultant disease. Ann Bot 11:333–348.

Bergero R, Charlesworth D, Filatov DA, Moore RC (2008) Defining regions and

rearrangements of the *Silene latifolia* Y chromosome. Genetics 178:2045–53.

Bernasconi G, Antonovics J, Biere A, Charlesworth D, Delph LF, Filatov D et al. (2009) *Silene* as a model system in ecology and evolution. Heredity (Edinb) 103:5–14.

Bremer, B., Bremer, K., Chase, M., Fay, M., Reveal, J., Soltis D et al., (2009) An update of the Angiosperm Phylogeny Group Classification for the orders and families of floweringplants: APG III. Bot J Linn Soc 161:105–121.

Buschmann C (2007) Variability and application of the chlorophyll fluorescence emission ratio red/far-red of leaves. Photosynth Res 92:261–71.

Calderon-Urrea A, Dellaporta SL (1999) Cell death and cell protection genes determine the fate of pistils in maize. Development 126:435–41.

Charlesworth D, Guttman DS (1999). The evolution of dioecy and plant sex chromosome systems. In Sex Determination in Plants. Edited by Ainsworth CC. pp 25-49. BIOS Scientific Publishers, Oxford, UK.

Charlesworth D (2002) Plant sex determination and sex chromosomes. Heredity (Edinb)

88:94–101.

Charlesworth D (2016) Plant Sex Chromosomes. Annu Rev Plant Biol 67:397–420.

Desfeux C, Maurice S, Henry JP, Lejeune B, Gouyon PH (1996) Evolution of reproductive systems in the genus Silene. Proc Biol Sci 263:409–14.

Daher A, Adam H, Chabrillange N, Collin M, Mohamed N, Tregear JW, et al. (2010) Cell cycle arrest characterizes the transition from a bisexual floral bud to a unisexual flower in *Phoenix dactylifera*. Ann Bot 106:255–66.

Denchev, CM, Giraud, T, Hood, ME (2009) Three new species of anthericolous smut fungi on Caryophyllaceae. Mycol Balc 6:79–84.

Diggle PK, Di Stilio VS, Gschwend AR, Golenberg EM, Moore RC, Russell JRW, et al. (2011) Multiple developmental processes underlie sex differentiation in angiosperms. Trends Genet 27:368–76.

Donnison IS, Siroky J, Vyskot B, Saedler H, Grant SR (1996) Isolation of Y chromosome-specific sequences from *Silene latifolia* and mapping of male sex-determining

genes using representational difference analysis. Genetics 144:1893–901.

Farbos I, Veuskens J, Vyskot B, Oliveira M, Hinnisdaels S, Aghmir A et al. (1999) Sexual dimorphism in white campion: deletion on the Y chromosome results in a floral asexual phenotype. Genetics 151:1187–96.

Fujita N, Torii C, Ishii K, Aonuma W, Shimizu Y, Kazama Y et al. (2012) Narrowing down the mapping of plant sex-determination regions using new Y-chromosome-specific markers and heavy-ion beam irradiation-induced Y-deletion mutants in *Silene latifolia*. G3 (Bethesda) 2:271–8.

Flores-Rentería L, Orozco-Arroyo G, Cruz-García F, García-Campusano F, Alfaro I, Vázquez-Santana S (2013) Programmed cell death promotes male sterility in the functional dioecious *Opuntia stenopetala* (Cactaceae). Ann Bot 112:789–800.

Garber ED, Ruddat M (2002) Transmission genetics of *Microbotryum violaceum* (*Ustilago violacea*): a case history. Adv Appl Microbiol 51:107–27.

Goldberg RB, Beals TP, Sanders PM (1993) Anther development: basic principles and

practical applications. Plant Cell 5:1217–1229.

Giraldo MC, Valent B (2013) Filamentous plant pathogen effectors in action. Nat Rev Microbiol 11:800–814.

Giraud T, Yockteng R, López-Villavicencio M, Refrégier G, Hood ME (2008) Mating system of the anther smut fungus *Microbotryum violaceum*: selfing under heterothallism. Eukaryot Cell 7:765–75.

Granberg A, Carlsson Graner U, Arnqvist P, Giles BE (2008) Variation in breeding system traits within and among populations of *Microbotryum violaceum* on *Silene dioica*. Int J Plant Sci 169:293–303.

Grant S, Hunkirchen B, Saedler H (1994) Developmental differences between male and female flowers in the dioecious plant *Silene latifolia*. Plant J 6:471–480.

Grasl-Kraupp B, Ruttkay-Nedecky B, Koudelka H, Bukowska K, Bursch W, Schulte-Hermann R (1995) *In situ* detection of fragmented DNA (TUNEL assay) fails to discriminate among apoptosis, necrosis, and autolytic cell death: a cautionary note.

Hepatology 21:1465–8.

Hao Y-J, Wang D-H, Peng Y-B, Bai S-L, Xu L-Y, Li Y-Q, et al. (2003) DNA damage in the early primordial anther is closely correlated with stamen arrest in the female flower of cucumber (*Cucumis sativus* L.). Planta 217:888–95.

Hardenack S, Ye D, Saedler H, Grant S (1994) Comparison of MADS box gene expression in developing male and female flowers of the dioecious plant white campion. Plant Cell 6:1775–1787.

Hobza R, Hrusakova P, Safar J, Bartos J, Janousek B, Zluvova J et al. (2006) MK17, a specific marker closely linked to the gynoecium suppression region on the Y chromosome in *Silene latifolia*. Theor Appl Genet 113:280–7.

Hood ME (2002) Dimorphic mating-type chromosomes in the fungus *Microbotryum violaceum*. Genetics 160:457–61.

Ishii K, Sugiyama R, Onuki M, Kazama Y, Matsunaga S, Kawano S (2008) The Y chromosome-specific STS marker MS2 and its peripheral regions on the Y chromosome of the dioecious plant *Silene latifolia*. Genome 51:251–60.

Kawamoto H, Yamanaka K, Koizumi A, Hirata A, Kawano S (2016) Cell Death and Cell Cycle Arrest of *Silene latifolia* Stamens and Pistils After *Microbotryum lychnidis-dioicae* Infection. Plant Cell Physiol DOI: 10.1093/pcp/pcw193.

Kazama Y, Koizumi A, Uchida W, Ageez A, Kawano S (2005) Expression of the floral B-function gene *SLM2* in female flowers of *Silene latifolia* infected with the smut fungus *Microbotryum violaceum*. Plant Cell Physiol 46:806–811.

Kazama Y, Ishii K, Aonuma W, Ikeda T, Kawamoto H, Koizumi A, Filatov DA, Chibalina M, Bergero R, Charlesworth D, Abe T, Kawano S (2016) A new physical mapping approach refines the sex-determining gene positions on the *Silene latifolia* Y-chromosome. Sci Rep 6:18917.

Kemler M, Göker M, Oberwinkler F, Begerow D (2006) Implications of molecular characters for the phylogeny of the Microbotryaceae (Basidiomycota: Urediniomycetes). BMC Evol Biol 6:35.

Kim JC, Laparra H, Calderón-Urrea A, Mottinger JP, Moreno MA, Dellaporta SL (2007) Cell

cycle arrest of stamen initials in maize sex determination. Genetics 177:2547–51.

Koizumi A, Amanai Y, Ishii K, Nishihara K, Kazama Y, Uchida W et al. (2007) Floral development of an asexual and female-like mutant carrying two deletions in gynoecium-suppressing and stamen-promoting functional regions on the Y chromosome of the dioecious plant *Silene latifolia*. Plant Cell Physiol 48:1450–61.

Koizumi A, Yamanaka K, Kawano S (2009) Carpel development in a floral mutant of dioecious *Silene latifolia* producing asexual and female-like flowers. J Plant Physiol 166:1832–8.

Koizumi A, Yamanaka K, Nishihara K, Kazama Y, Abe T, Kawano S (2010) Two separate pathways including *SlCLV1*, *SlSTM* and *SlCUC* that control carpel development in a bisexual mutant of *Silene latifolia*. Plant Cell Physiol. 51: 282-293.

Lebel-Hardenack S, Hauser E, Law TF, Schmid J, Grant SR (2002) Mapping of sex determination loci on the white campion (*Silene latifolia*) Y chromosome using amplified fragment length polymorphism. Genetics 160:717–25.

Li N, Zhang D-S, Liu H-S, Yin C-S, Li X, Liang W, et al. (2006) The rice tapetum degeneration retardation gene is required for tapetum degradation and anther development. Plant Cell 18:2999–3014.

Matsunaga S, Uchida W, Kawano S (2004) Sex-specific cell division during development of unisexual flowers in the dioecious plant *Silene latifolia*. Plant Cell Physiol 45:795–802.

Matsuo Y, Arimura S, Tsutsumi N (2013) Distribution of cellulosic wall in the anthers of *Arabidopsis* during microsporogenesis. Plant Cell Rep 32:1743–50.

Meyberg M (1988) Selective staining of fungal hyphae in parasitic and symbiotic plant-fungus associations. Histochemistry 88:197–9.

Mitchell CH, Diggle PK (2005) The evolution of unisexual flowers: morphological and functional convergence results from diverse developmental transitions. Am J Bot 92:1068–76.

Moore RC, Kozyreva O, Lebel-Hardenack S, Siroky J, Hobza R, Vyskot B et al. (2003) Genetic and functional analysis of DD44, a sex-linked gene from the dioecious plant *Silene latifolia*, provides clues to early events in sex chromosome evolution. Genetics 163:321–34.

Nakao S, Matsunaga S, Sakai A, Kuroiwa T, Kawano S (2002) RAPD isolation of a Y chromosome specific ORF in a dioecious plant, *Silene latifolia*. Genome 45:413–420.

Pacini E, Franchi GG, Hesse M (1985) The tapetum: Its form, function, and possible phylogeny in Embryophyta. Plant Syst Evol 149:155–185.

Papini A, Mosti S, Brighigna L (1999) Programmed-cell-death events during tapetum development of angiosperms. Protoplasma 207:213–221.

Piepenbring M, Bauer R, Oberwinkler F (1998) Teliospores of smut fungi general aspects of teliospore walls and sporogenesis. Protoplasma 204:155–169.

Pintozzi RL (1978) Modified Grocott's methenamine silver nitrate method for quick staining of Pneumocystis carinii. J Clin Pathol 31:803–5.

Renner SS (2014) The relative and absolute frequencies of angiosperm sexual systems: Dioecy, monoecy, gynodioecy, and an updated online database. Am J Bot 101:1588–1596.

Schäfer AM, Kemler M, Bauer R, Begerow D (2010) The illustrated life cycle of *Microbotryum* on the host plant *Silene latifolia*. Botany 88:875–885.

Sanders PM, Bui AQ, Weterings K, McIntire KN, Hsu Y-C, Lee PY, et al. (1999) Anther developmental defects in *Arabidopsis thaliana* male-sterile mutants. Sex Plant Reprod 11:297–322.

Scotti I, Delph LF (2006) Selective trade-offs and sex-chromosome evolution in *Silene latifolia*. Evolution (N Y) 60:1793–1800.

Sorensen A, Guerineau F, Canales-Holzeis C, Dickinson HG, Scott RJ (2002) A novel extinction screen in *Arabidopsis thaliana* identifies mutant plants defective in early microsporangial development. Plant J 29:581–594.

Strittmatter LI, Negrón-Ortiz V, Hickey JR (2006) Comparative microsporangium development in male-fertile and male-sterile flowers of *Consolea* (Cactaceae): When and how does pollen abortion occur. Grana 45:81–100.

Uchida W, Matsunaga S, Sugiyama R, Kazama Y, Kawano S (2003) Morphological

development of anthers induced by the dimorphic smut fungus *Microbotryum violaceum* in female flowers of the dioecious plant *Silene latifolia*. Planta 218:240–248.

Uchida W, Matsunaga S, Kawano S (2005) Ultrastructural analysis of the behavior of the dimorphic fungus Microbotryum violaceum in fungus-induced anthers of female Silene latifolia flowers. Protoplasma 226:207–216.

Warmke HE (1946) Sex determination and sex balance in *Melandrium*. Am J Bot 33:648.

Wu HM, Cheun AY (2000) Programmed cell death in plant reproduction. Plant Mol Biol 44:267–281.

Yang S-L, Xie L-F, Mao H-Z, Puah CS, Yang W-C, Jiang L, et al. (2003) Tapetum determinant1 is required for cell specialization in the *Arabidopsis* anther. Plant Cell 15:2792–804.

Zhang W, Sun Y, Timofejeva L, Chen C, Grossniklaus U, Ma H (2006) Regulation of *Arabidopsis* tapetum development and function by DYSFUNCTIONAL TAPETUM1 (DYT1) encoding a putative bHLH transcription factor. Development 133:3085–95.

APPENDIX

Location of gold particles and puncture of tobacco leaf epidermis by particle bombardment

SUMMARY

Scanning electron microscopy (SEM) is used to observe surface structures. The electron beam generally scans the cell surface at an acceleration voltage of 10–15 kV. I observed buried gold particles in cells at an acceleration voltage of 30 kV. In this paper, dim, opaque particles were observed on a leaf surface that was bombarded with gold particles using a particle gun. These gold particles were buried in epidermal cells and the outline of the particle was not clear compared to adhered particles on the leaf surface. A 1-μm hole (0.785 μm^2 in area) made by a 1-μm gold particle was observed around the buried particle. I measured the areas of holes made by the passage of gold particles at 1 min (n = 61), 2 min (n = 56), 5 min (n = 110), and 10 min (n = 61) after bombardment using images obtained using a scanning electron microscope and ImageJ software. The size of the holes became smaller over time and was very small 10 min after bombardment. From these results, I reveal that the holes formed by gold particle bombardment are repaired after about 10 minutes.

INTRODUCTION

Plant transformation is an important tool for plant breeding and the study of plant biology. Transformation methods, such as *Agrobacterium*-mediated transformation (Hooykaas and Schilperoort, 1992; Tepfer, 1990; Zupan and Zambryski, 1995), electroporation (Fromm *et al.*, 1985; D'Halluin *et al.*, 1992), polyethylene glycol mediated transformation (Hayashimoto *et al.*, 1990; O'Neill *et al.*, 1993), and particle bombardment (Bower and Birch, 1992; Christou *et al.*, 1991), were developed to produce transgenic plants.

Particle bombardment transforms plants by shooting gold particles coated with DNA into cells. This method is used more extensively than the other transformation methods, regardless of cell type. In addition, this method is simple and takes less time than the microinjection method. It is convenient for the transformation of intact culture cells, requiring less before and after bombardment treatment. In a recent study, transformation using *in vitro* particle bombardment was reported in sensitive animal culture cells, which are difficult to transform by chemical methods such as lipofection and electroporation (Ma *et al.*, 2003; Morín *et al.*, 2009). There are also examples of RNA introduced into cells (Vassilev *et al*., 2001; Kennerdel *et al*., 2002) and siRNA introduced into skin (Kim *et al*., 2005). In spite of the large number of experiments, it is not clear how the bombarded gold particles are taken up in the cell.

Scanning electron microscopy (SEM) is used to observe surface structure. A secondary electron is released by the sample surface when it is irradiated with an electron beam. A detector detects the secondary electron and an SEM image is created based on the quantity of secondary electrons, indicating brightness. SEM produces an image of the sample surface because the quantity of secondary electrons changes with regard to the texture of the sample surface. The electron beam is produced by an electron source and is accelerated by an electron gun. The electron invasion depth also changes with changes in the acceleration voltage. The higher the acceleration voltage, the deeper the depth is. Therefore, I can obtain information on the sample interior. Usually, the electron beam scans cell surfaces at an acceleration voltage of 10–15 kV; however, I observed buried gold particles in cells at an acceleration voltage of 30 kV. In this paper, I observed holes and bombarded gold particles in epidermal cells of *Nicotiana benthamiana* using a scanning electron microscope set at an acceleration voltage of 30 kV.

MATERIALS AND METHODS

Plant materials and plant growth conditions

Nicotiana benthamiana plants were grown at 25°C with a 16-h light/8-h dark photoperiod. The sixth or seventh true leaves of four- to five-week-old *N.benthamiana* plants were bombarded *in planta* with 1-μm gold particles (Bio-Rad Laboratories) using the Helios Gene

Gun System according to manufacturer's instructions (Bio-Rad Laboratories). The firing pressure was 150–250 psi, which was optimal for transient expression of a green fluorescent protein reporter gene introduced into the epidermal cells together with the gold particles (data not shown).

Scanning electron microscopy (SEM)

Leaves were fixed overnight in 2.5% glutaraldehyde in 0.1 M phosphate buffer (pH 7.2) at 4℃. After being washed three times with 0.1 M phosphate buffer (pH 7.2), fixed flowers were dehydrated in an ethanol series (30%, 50%, 70%, 80%, 90%, 95%, and 100% each step for 30 min at room temperature) and maintained in 100% ethanol overnight at 4℃. The ethanol treatment was replaced with isopentyl acetate and the leaves were dried using a critical-point dryer (HCP-2, Hitachi, Tokyo) and sputter-coated with platinum–palladium using an ion sputter (E-1010, Hitachi). The leaves were examined on an S-3000N SEM (Hitachi) operated at 15 kV and 30kV in the high vacuum mode. I measured the areas of holes made by the passage of gold particles using ImageJ software.

Results

Observation of adhered gold particles and buried gold particles using a scanning electron microscope

I observed a leaf surface, which was bombarded by gold particles, using a scanning electron microscope. Guard cells and jigsaw puzzle-like epidermal cells were observed on the leaf surface. I observed both the leaf surface and chloroplasts near the epidermis at a 30-kV acceleration voltage. A high brightness particle was observed on a leaf bombarded by 1-μm gold particles (Fig. 1a). This high brightness particle was stuck to the leaf surface because it was not able to pass through the cell wall. A dim, opaque particle was also observed. This gold particle was buried in an epidermal cell; therefore the outline of the particle was not clear compared with the adhered particle on the leaf surface. A 1-μm hole (0.785 μm^2 in area) made by a 1-μm gold particle was observed around the buried particle (Fig. 1b, c). I think that this gold particle passed through the cell wall with minimal destruction because the particle and hole were the same size and the hole formed a perfect circle.

Observation of hole repair on* N. benthamiana *leaf surfaces.

I observed the repair process of holes produced by gold particle bombardment into tobacco leaves (Fig. 2). Most of the holes were 1-μm perfect circles (0.785 μm^2 in area) produced by passage of the gold particle after bombardment (Fig. 2a). Both small and large (0.785 μm^2 in area) holes were observed. Small holes are produced by reflected gold particles on the leaf surface, while large holes are produced by the strong shock of bombarding gold particles (Fig. 3). I think that the holes (Fig. 2a) were produced by gold particles because the

size of the particles was 1 μm. When I observed the subsequent repair 5 min after bombardment, I found that a fibrous structure had formed on the inside of the hole (Fig. 2b). At this point, the original perfect circle was oval-shaped due to the fibrous structure on the edge of the hole (Fig. 2c). Ten minutes after bombardment, the hole was around one-tenth of its original size compared to 1 min after bombardment (Fig. 2d).

Due to the change in shape from a circle to an oval, I measured the area rather than the diameter to examine the repair process. I measured holes at 1 min (n = 61), 2 min (n = 56), 5 min (n = 110), and 10 min (n = 61) after bombardment and obtained images using a scanning electron microscope and ImageJ software (Fig. 3). The area of the 1-μm holes, which is the same size as a gold particle, was approximately 0.785 μm^2. However, large holes and small holes, both of which are about 0.785 μm^2, were present 1 min after bombardment (Fig. 3a). I think that small holes were produced by reflected gold particles that were not able to penetrate the surface, but left a wound. In addition, I think that large holes were produced by the strong shock of bombarding gold particles or oblique hits. Two minutes after bombardment, there were no significant differences compared to 1 min (Fig. 3b). At 5 min after bombardment, most holes were smaller than 0.785 μm^2 and were mainly 0.1–0.4 μm^2 (Fig. 3c). At 10 min after bombardment, most holes were 0.1–0.2 μm^2 (Fig. 3d). The holes became smaller over time and were very small 10 min after bombardment. Most holes appeared to be repaired after about 10 min.

DISCUSSION

In this paper, I observed the repair process of holes formed on tobacco leaves by the bombardment of gold particles from a particle gun. A fibrous structure formed in the holes over time (Fig. 2b). Plant cells are surrounded by a cell wall of cellulose microfibrils (Wolf *et al.*, 2012). Cellulose is a linear macromolecule and cellulose microfibrils are formed by bundling of cellulose through hydrogen bonds. Usually, cellulose microfibrils are arranged in parallel to form the framework of the cell wall. Xyloglucan endotransglucosylase/hydrolase (XTH) plays a central role in the crosslinking and decomposition of cellulose microfibrils and in the formation and maintenance of cell wall structure (Rose *et al.*, 2002;). It is thought that XTH plays a role in maintaining thickness while incorporating new cellulose microfibrils in growing cell walls and restoring cell walls by catalyzing the transfer reaction of crosslinks of cellulose microfibrils (Nishitani and Vissenberg, 2007). I think that cellulose microfibrils fill the bombardment hole as a scaffold (Fig. 2).

Particle bombardment produces transient transformants and stable transformants in many animals and plants (Birch, 1997), but the transformation efficiency of particle bombardment is not high. Five transient transformants were obtained after bombardment by approximately 8,000 particles per dish with a particle gun (Julie R Kikkert, José R Vidal *et al.*, 2005). Many holes, around 1 μm in size, were detected 1 min after bombardment (Fig. 3).

Only six particles were seen on the inside of the leaf, whereas 30 particles were attached to the leaf surface, though gold particles may have been washed away during fixation or dehydration (Fig. 1). I think that small holes were produced by reflected gold particles on the leaf surface and large holes were made by the strong shock of bombarding gold particles or oblique hits. It is possible that the low transformation efficiency of particle bombardment is due to the reflected particles on the leaf and wounds made by the strong shock of bombarding gold particles or oblique hits.

ACKNOWLEDGEMENTS

This work was performed as part of a Laboratory Course for Broadened Bioscience Skills in Laboratory of Plant Life System, The University of Tokyo.

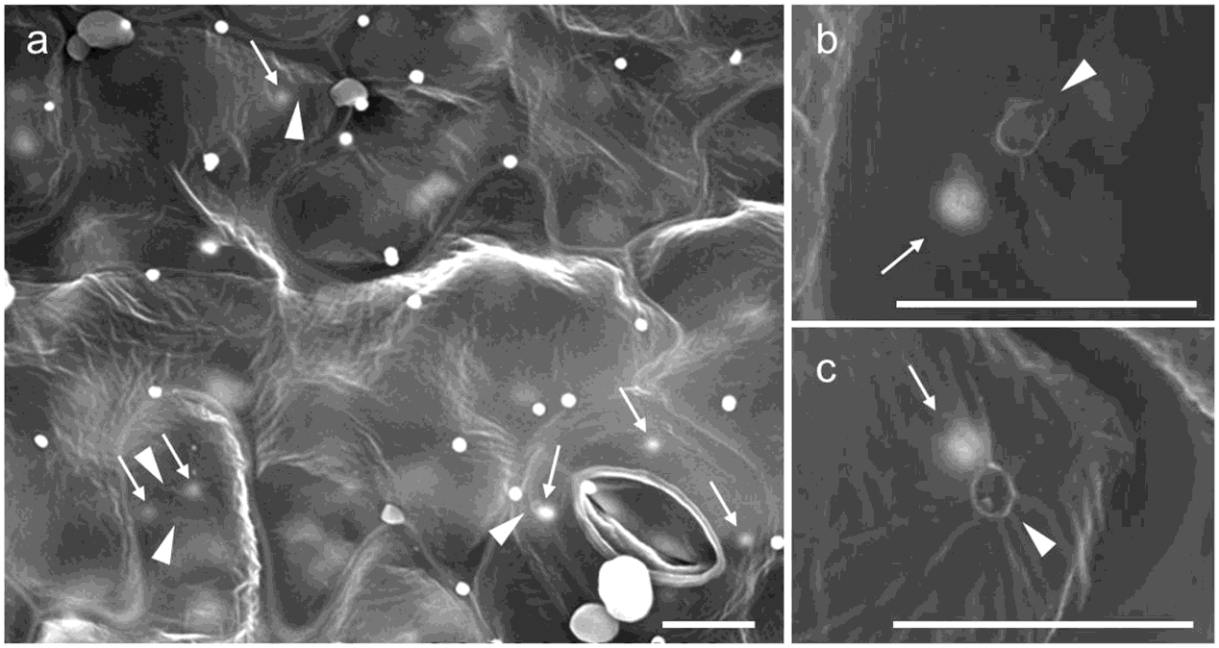

Fig. 1 Scanning electron micrographs of a leaf shot by a particle gun. Arrowheads indicate holes made by gold particles. White arrows indicate gold particles in plants. Bars = 10 μm.

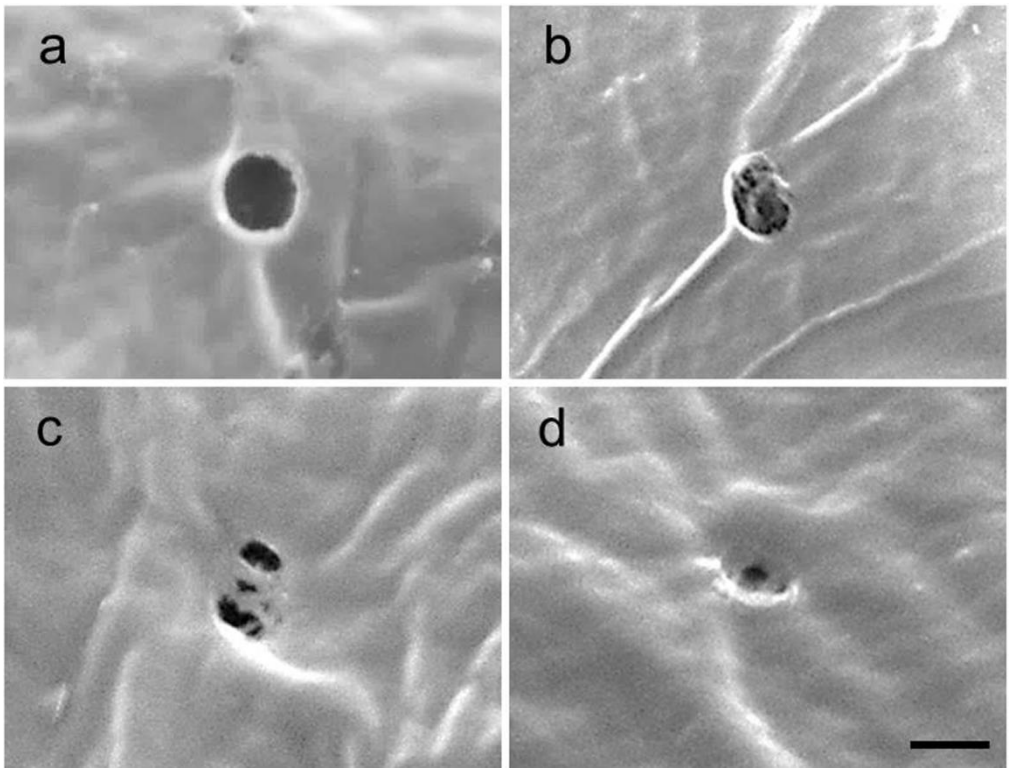

Fig. 2 Scanning electron micrographs of the repair process of holes in leaves. The repair of holes in tobacco leaves was observed using a scanning electron microscope. Bar = 1 μm.

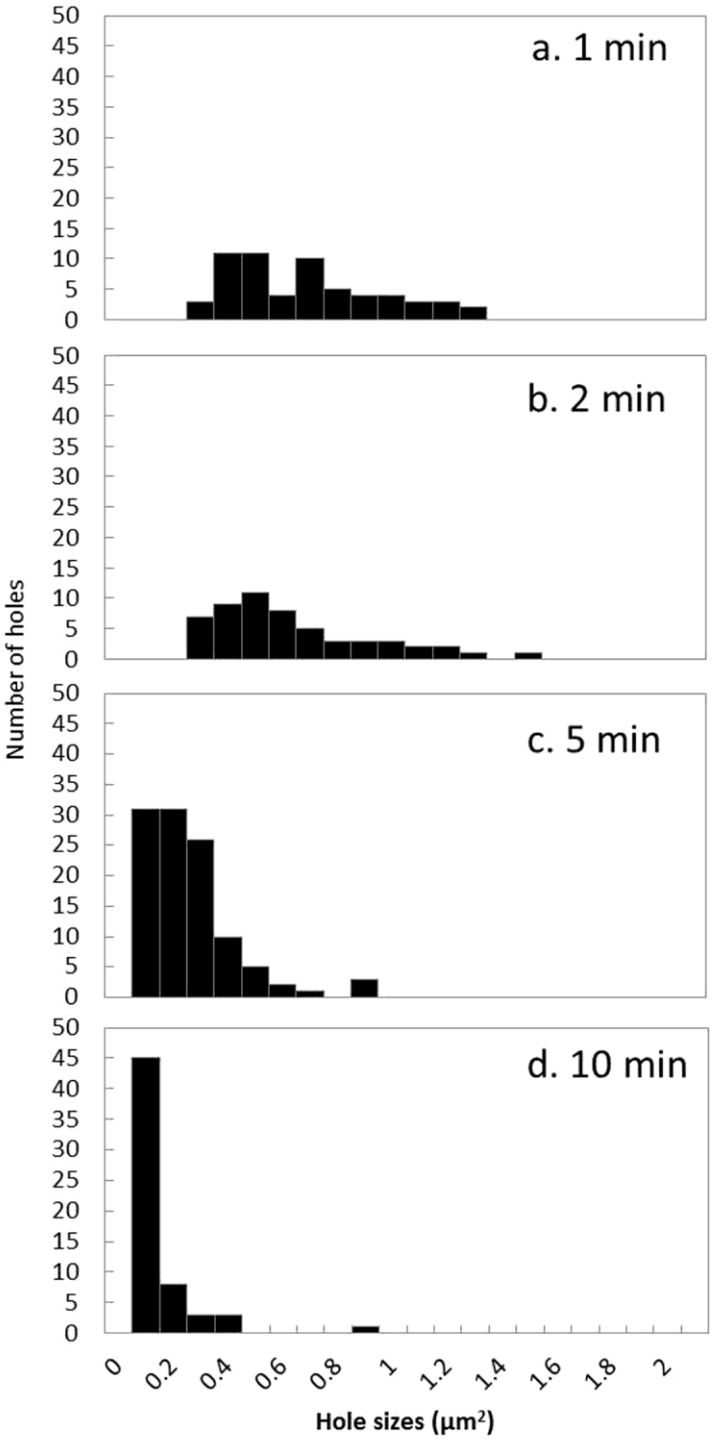

Fig. 3 Histograms of the repair process of holes in leaves. I measured the areas of the holes produced by the gold particles at 1 min (n = 61), 2 min (n = 56), 5 min (n = 110), and 10 min after bombardment (n = 61) and acquired images using a scanning electron microscope and ImageJ software.

Reference

Birch, R. G. 1997. PLANT TRANSFORMATION: Problems and Strategies for Practical Application. Annu. Rev. Plant Physiol.

Plant Mol. Biol. 48: 297–326. Bower, R. and Birch, R. G. 1992. Transgenic sugarcane plants via microprojectile bombardment. Plant J. 2: 409–416.

Christou, P., Ford, T. L. and Kofron, M. 1991. Production of transgenicrice (Oryza sativa L.) plants from agronomically important indica and japonica varieties via electric discharge particle acceleration of exogenous DNA into immature zygotic embryos. Nat. Biotechnol. 9: 957–962.

D'Halluin, K., Bonne, E., Bossut, M., De Beuckeleer, M. and Leemans, J. 1992. Transgenic maize plants by tissue electroporation. Plant Cell 4: 1495–1505.

Fromm, M., Taylor, L. P. and Walbot, V. 1985. Expression of genes transferred into monocot and dicot plant cells by electroporation. Proc. Natl. Acad. Sci. U.S.A. 82: 5824–5828.

Hayashimoto, A., Li, Z. and Murai, N. 1990. A polyethylene glycolmediated protoplast

transformation system for production of fertile transgenic rice plants. Plant Physiol. 93: 857–863.

Hooykaas, P. J. and Schilperoort, R. A. 1992. Agrobacterium and plant genetic engineering. Plant Mol. Biol. 19: 15–38.

Kennerdell, J. R., Yamaguchi, S. and Carthew, R. W. 2002. RNAi is activated during Drosophila oocyte maturation in a manner dependent on aubergine and spindle-E. Genes Dev. 16: 1884–1889.

Kikkert, J. R., Vidal, J. R. and Reisch, B. I. 2005. Stable transformation of plant cells by particle bombardment/biolistics. Methods Mol. Biol. 286: 61–78.

Kim, T. W., Lee, J. H., He, L., Boyd, D. A., Hardwick, J. M., Hung, C. F. and Wu, T. C. 2005. Modification of professional antigenpresenting cells with small interfering RNA in vivo to enhance cancer vaccine potency. Cancer Res. 65: 309–316.

Ma, X. M., Huang, J., Wang, Y., Eipper, B. A. and Mains, R. E. 2003. Kalirin, a multifunctional Rho guanine nucleotide exchange factor, is necessary for maintenance of

hippocampal pyramidal neuron dendrites and dendritic spines. J. Neurosci. 23: 10593–10603.

Morín, M., Bryan, K. E., Mayo-Merino, F., Goodyear, R., Mencia, A., Modamio-Høybjør, S., del Castillo, I., Cabalka, J. M., Richardson, G., Moreno, F., Rubenstein, P. A. and Moreno-Pelayo, M. A. 2009. In vivo and in vitro effects of two novel gamma-actin (ACTG1) mutations that cause DFNA20/26 hearing impairment. Hum. Mol. Genet. 18: 3075–3089.

Nishitani, K. and Vissenberg, K. 2007. Roles of the XTH protein family in the expanding cell. Plant Cell Monogr. 6: 89–116.

O'Neill, C., Horváth, G. V., Horváth, E., Dix, P. J. and Medgyesy, P. 1993. Chloroplast transformation in plants: Polyethylene glycol (PEG) treatment of protoplasts is an alternative to biolistic delivery systems. Plant J. 3: 729–738.

Rose, J. K., Braam, J., Fry, S. C. and Nishitani, K. 2002. The XTH family of enzymes involved in xyloglucan endotransglucosylation and endohydrolysis: Current perspectives and a new unifying nomenclature. Plant Cell Physiol. 43: 1421–1435.

Tepfer, D. 1990. Genetic transformation using Agrobacterium rhizogenes. Physiol. Plant. 79:

140–146.

Vassilev, V. B., Gil, L. H. and Donis, R. O. 2001. Microparticlemediated RNA immunization against bovine viral diarrhea virus. Vaccine 19: 2012–2019.

Wolf, S., Hematy, K. and Hofte, H. 2012. Growth control and cell wall signaling in plants. Annu. Rev. Plant Biol. 63: 381–407.

Zupan, J. R. and Zambryski, P. 1995. Transfer of T-DNA from Agrobacterium to the plant cell. Plant Physiol. 107: 1041–1047.